Optical orientation of excitons in hybrid metal-semiconductor nanostructures

A. V. Korotchenkov * and N. S. Averkiev
Ioffe Institute, Politechnicheskaya 26, St. Petersburg 194021, Russian Federation

(Received 5 December 2023; revised 5 March 2024; accepted 7 March 2024; published 18 March 2024)

We demonstrate the possibility of the optical orientation of excitons in the near field of the metal grating that covers a semiconductor nanostructure. Excitons generated this way have the wave vector greater than the wave vector of the incident radiation. We suggest that optical orientation method is applicable to study the fine structure and kinetics of the hot excitons in semiconductor quantum well.

DOI: 10.1103/PhysRevB.109.125418

I. INTRODUCTION

Principles of optical orientation and alignment, which were initially developed for atomic gases, are widely employed in the spectroscopy of excitons in semiconductors [1,2]. In addition to the exitons in bulk crystals [3], these methods allow investigating the fine structure of excitons in semiconductor nanostructures and estimating the exciton lifetime and spin relaxation time [4,5]. Normally one generates the excitons with polarized light at the resonance frequency ω_0, and measures the polarization of luminescence due to direct optical transitions. This way, either free excitons with small wave vectors $\boldsymbol{K} \approx 0$, which they obtain from the incident light, or the localized excitons are studied. In bulk semiconductors, orientation of hot excitons that have significant $\boldsymbol{K}$ and kinetic energy is only attainable through indirect transitions accompanied by the optical phonon emission [6]. On the other hand, it is possible to fabricate a metallic grating that supports the surface plasmon polaritons (SPPs) on top of a semiconductor heterostructure and preserve the exciton resonance [7]. In the resulting hybrid nanostructure, excitons acquire the wave vector and polarization (spin) of SPPs that propagate along the grating [8]. This means, in principle, that one could study the properties of excitons with nonzero wave vectors by exciting them through the grating and measuring their polarized luminescence.

In the present paper, we consider the orientation of excitons in a hybrid nanostructure that consists of a semiconductor quantum well (QW) and a square grating of metal nanoparticles (NPs). For instance, similar structures including the ZnO QW and Ag nanodisks were fabricated to investigate the coupling between localized surface plasmons and semiconductor excitons [9]. We have considered the plasmon-exciton coupling and estimated its effect on the optical spectra of such systems previously [10]. Since we propose applying the grating to study hot excitons, we consider the weak-coupling regime, which is realistic in case of the Wannier-type excitons and localized surface plasmons. Strong plasmon-exciton coupling and related effects were observed for either molecular excitons in organic dyes [11], or for small-radius excitons in TMDCs [12,13]. In these systems, properties of the excitations are strongly modified by the plasmon-exciton hybridization.

The paper is organized in the following way. In Sec. II, we find the electric field scattered by the grating, approximating the nanoparticles by discrete electric dipoles. A concise description of this model and its applications can be found in [14]. Polarization of the near field they produce inside the QW is quite different from polarization of the incident electromagnetic wave. Next, we calculate the exciton generation matrix that enters the kinetic equation, which we solve in Sec. III to obtain the stationary exciton density matrix. At this stage, we consider the effect of the stationary homogeneous magnetic field applied perpendicularly to the QW plane. Since the grating allows simultaneously generating excitons that propagate in different directions, we take into account both exciton spin and exciton momentum relaxation. In Sec. IV, we calculate the polarization of secondary radiation of the excitons facilitated by the grating. In Sec. V, we show how the energy relaxation can be included in the kinetic equation for excitons and discuss its effect on the polarized luminescence. As the principal result, we find out how the luminescence polarization varies with the applied magnetic field, and demonstrate that the hybrid nanostructures make it possible to study the kinetic characteristics of the hot excitons.

II. GENERATION OF EXCITONS THROUGH THE GRATING

Consider a structure shown in Fig. 1, which contains a semiconductor quantum well (QW) and a grating of metallic nanoparticles (NPs). We assume the photon energy of the incident radiation close to the energy of excitonic transition in the QW, and the distance h between the grating and the QW less than the wavelength in semiconductor. Then the excitons are generated by the near field of metallic grating, which results from scattering of the incident beam represented by the plane wave with a certain polarization tensor. To capture the essence of the optical orientation and alignment effects, we employ a commonly used model of exciton transitions shown in Fig. 2. Semiconductor QWs are known to support the Wannier-Mott excitons, whose binding energy is much smaller than the gap between electron subbands, and whose radius exceeds

*coalex@mail.ioffe.ru

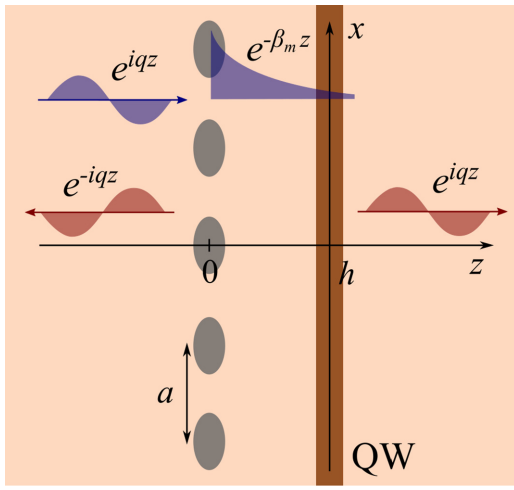

FIG. 1. Schematic of nanostructure consisting of a semiconductor quantum well (QW) and a short-period grating of metal nanoparticles (NPs).

the crystal lattice period due to the relatively large dielectric permittivity and small effective masses of charge carriers. In this case, the exciton wave function is a product of the smooth envelope $F(\boldsymbol{r}_e, \boldsymbol{r}_h)$ that depends on the electron and hole coordinates, and the Bloch functions (X, Y, Z, and S), which correspond to the top of the valence band and the bottom of the conduction band [15]. The envelope in turn is the product of the function $\varphi(\boldsymbol{\rho}_e - \boldsymbol{\rho}_h, z_e, z_h)$ describing the relative motion of electron and hole, and the exponent $\exp(i\boldsymbol{K}\cdot\boldsymbol{\rho})$ that corresponds to the propagation of exciton along the QW plane. In bulk semiconductors with the zinc-blende structure, like GaAs, electron states at the top of the valence band are fourfold degenerate, resembling the states with the total angular momentum $\mathcal{J} = 3/2$. However, in QWs this degeneracy is lifted due to the lower symmetry, and states with the projection of the angular momentum on the growth axis $j = \pm 3/2$ or $j = \pm 1/2$ give rise to the separate subbands. In sufficiently narrow QWs the upper valence subband is formed by the

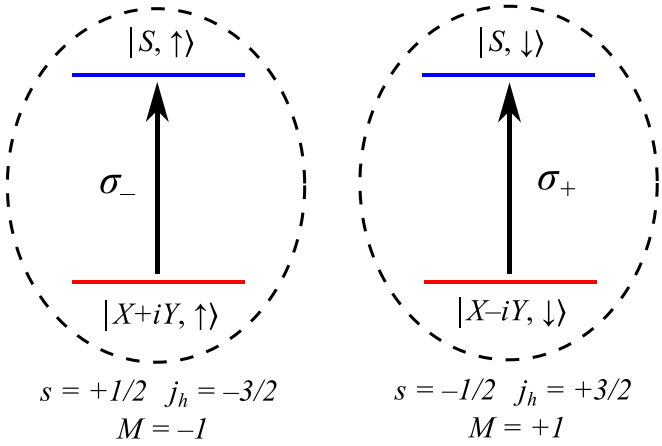

FIG. 2. Optically active exciton states formed by conduction band electrons and heavy holes in the valence band. Electron states are labeled with the Bloch function S or $X \pm iY$ and spin $\uparrow$ or $\downarrow$. Excitons with spin $M = -1$ or $+1$ interact with the left or right circularly polarized light correspondingly.

heavy hole states corresponding to $j = \pm 3/2$. The binding energy of the heavy hole exciton is smaller than the energy gap between the heavy and the light hole ($j = \pm 1/2$) subbands, which results from the size quantization. Therefore, the light hole mixing can be neglected as we consider the lowest band of the excitons, formed by the heavy holes ($j = \pm 3/2$) and the conduction band electrons with the spin projection $s = \pm 1/2$. Thus, we have four possible states of excitons that differ in the projection of the total spin on the growth axis $M = \pm 1, \pm 2$. Excitons with the spin projection ± 1 are optically active, while states with the spin projection ± 2 are optically inactive and therefore can be omitted. Optically active (bright) and inactive (dark) excitons can hybridize due to exchange interaction, which plays significant role in the orientation of localized excitons [16], but we do not take this effect into account here.

According to the selection rules shown in Fig. 2, light with circular polarization σ_+ generates the excitons with spin projection $M = +1$, while σ_--polarized light generates the excitons with $M = -1$. Then the secondary radiation of excitons partially retains the circular polarization of incident beam. Linearly polarized light (we define the polarization in the QW plane xy) generates the superposition of exciton states ± 1 such that the total spin is oriented along the x or y axis, which is called the optical alignment effect. The radiation from recombination of excitons in this state is also linearly polarized. An external magnetic field oriented along z axis splits the states with $M = \pm 1$ and reduces the coherence of superposition states, which decreases the linear polarization of exciton radiation. Measurements of the dependence of luminescence polarization on the strength or direction of magnetic field provide estimations of exciton relaxation times and of the g-factor value for excitons.

This simple picture is suitable for a structure with no grating, where incident light generates only excitons with near-zero wave vectors $\boldsymbol{K}$ in the QW plane. Now we consider a square lattice of conducting NPs, such that the surface plasmon frequency lies in the same range as the frequency of exciton transition in the QW. The lattice is chosen square so that it does not introduce additional polarization to the incident radiation and does not alter the polarization of light emitted by the excitons with $\boldsymbol{K} = 0$. We suppose that the grating does not affect the intrinsic properties of excitons, such as binding energy and dipole moment, which are defined by the relative motion of an electron and hole. In principle, the presence of the metal surfaces that produce the image charges should modify the Coulomb interaction between the electron and hole. However, the calculations for a QW with a spherical NP nearby [17] suggest that its effect on the exciton becomes substantial only for the few-nanometer distance h. Thus, the image charges can be neglected if the thickness of the barrier separating the NPs from the QW is larger than the exciton radius.

To calculate the field of nanoparticles, we use the discrete dipole approximation [18], which yields the total electric field in the following form:

$$\boldsymbol{E}(\boldsymbol{\rho}, z) = \boldsymbol{E}^0 \exp(iqz) + \sum_{\boldsymbol{m}} \boldsymbol{E}_{\boldsymbol{m}} \exp\left(i\boldsymbol{b}_{\boldsymbol{m}}\cdot\boldsymbol{\rho} + iq_{z,\boldsymbol{m}}|z|\right),$$

$$\boldsymbol{E}_{\boldsymbol{m}} = \frac{iq^2 b^2}{2\pi n^2 q_{z,\boldsymbol{m}}} \hat{G}(\boldsymbol{b}_{\boldsymbol{m}} + \mathrm{sgn}z\, q_{z,\boldsymbol{m}}\boldsymbol{e}_z)\mathcal{X}(\omega)\,\boldsymbol{E}^0. \qquad (1)$$

This equation contains the sum of the scattered waves that have the wave vector components $\boldsymbol{q}_\parallel$ in the grating plane $\boldsymbol{\rho} = (x, y)$ equal to the reciprocal lattice vectors $\boldsymbol{b_m} = b(m_x\boldsymbol{e}_x + m_y\boldsymbol{e}_y)$, where $b = 2\pi/a$, a is the lattice period. In case of the short-period grating that we intend to consider, the length of the vectors $\boldsymbol{b_{m\neq 0}}$ exceeds the wave number $q = n\omega/c$ of light propagating in the semiconductor with refractive index n. Therefore, the wave numbers $q_{z,\boldsymbol{m}} = (q^2 - \boldsymbol{b}_{\boldsymbol{m}}^2)^{1/2} = i\beta_{\boldsymbol{m}}$ are purely imaginary, and the corresponding waves decay exponentially along the direction z perpendicular to the grating. Amplitudes of the scattered waves are determined in the dipole approximation by the effective polarizability of NPs in the lattice $\mathcal{X}(\omega)$ and the tensor $\hat{G}(\boldsymbol{q}) = \boldsymbol{e}_s \otimes \boldsymbol{e}_s + \boldsymbol{e}_p \otimes \boldsymbol{e}_p$ that describes the radiation of electric dipole. This notation involves the tensor products of polarization vectors $\boldsymbol{e}_s = [\boldsymbol{e}_z \times \boldsymbol{q}_\parallel]/q_\parallel$ and $\boldsymbol{e}_p = [\boldsymbol{e}_s \times \boldsymbol{q}]/q$, whose definitions are extended to the region of evanescent waves $q_\parallel > q(\omega)$.

Since the wave vector component parallel to the QW is conserved in the optical transitions, the field of the lattice (1) can produce the excitons with wave vectors $\boldsymbol{K} = \boldsymbol{b_m}$. At the same time, the exciton transition energy $\mathcal{E}_{\rm exc}(K) \approx \mathcal{E}_{\rm exc}(0) + \hbar^2K^2/2M_{\rm exc}$, where $M_{\rm exc}$ is the exciton effective mass, must be close to the energy of the incoming photons. Optical transitions are characterized by the matrix element of the interaction operator $V_{\boldsymbol{K},M} = \langle \mathrm{exc}_{\boldsymbol{K},M}| - \int \hat{\boldsymbol{d}}(\boldsymbol{r}) \cdot \boldsymbol{E}\, d^3\boldsymbol{r}|0\rangle$, which we calculate using the smooth envelope approximation for the exciton wave function, see Sec. 2.7.5 of the book [15]. The density of the transition dipole moment $\langle \mathrm{exc}_{\boldsymbol{K},M}|\hat{\boldsymbol{d}}(\boldsymbol{r})|0\rangle = -ie/(m_0\omega_0)\ \boldsymbol{p}_M F^*_{\boldsymbol{K}}(\boldsymbol{r},\boldsymbol{r})$ is expressed via the wave function envelope with coinciding electron and hole coordinates, the interband matrix element of the momentum operator $\boldsymbol{p}_M$, charge e, and mass m_0 of a free electron. For simplicity, we assume that the exciton spin states are independent of its wave vector $\boldsymbol{K}$, therefore they are labeled with the same projection M as the states with $\boldsymbol{K} = 0$. Given that the envelope function may be written as $F_{\boldsymbol{K}}(\boldsymbol{r},\boldsymbol{r}) = S^{-1/2}\exp(i\boldsymbol{K}\cdot\boldsymbol{\rho})\Phi(z-h)$, where S is the QW area and $\Phi(z-h) = \varphi(0,z,z)$, after integrating the dipole moment density with the electric field (1) we obtain

$$V_{\boldsymbol{K},M} = (2\pi)^2 S^{-\frac{1}{2}} \sum_{\boldsymbol{m}} \delta(\boldsymbol{K} - \boldsymbol{b_m}) \int \Phi^*(z-h) e^{iq_{z,\boldsymbol{m}}z} dz \times \frac{ie}{m_0\omega_0} \boldsymbol{p}_M \left[\delta_{\boldsymbol{m},0} + \frac{iq^2b^2}{2\pi n^2 q_{z,\boldsymbol{m}}} \mathcal{X} \hat{G}_{\boldsymbol{b_m}}\right] \boldsymbol{E}^0. \quad (2)$$

The delta function $\delta(\boldsymbol{K} - \boldsymbol{b_m})$ indicates the conservation of the wave vector component in the QW plane, which assumes the values of the reciprocal lattice vectors $\boldsymbol{b_m}$. The overlap integral with even function $\Phi(z-h)$ entering the Eq. (2) was estimated in [10] for thin QWs, and can be deemed virtually independent of the wave number $q_{z,\boldsymbol{m}}$. The selection rules concerning the exciton spin are defined by the matrix element $\boldsymbol{p}_M$ calculated on the Bloch functions of the bands that form the exciton. As discussed before, we consider the case $\boldsymbol{p}_M = p_{\rm cv}\,\boldsymbol{e}^*_M$ for $M = \pm 1$, where $\boldsymbol{e}_\pm = (\boldsymbol{e}_x \pm i\boldsymbol{e}_y)/\sqrt{2}$ are the unit vectors of circular polarization, and $\boldsymbol{p}_{M=\pm 2} = 0$.

Now we can obtain the generation matrix, that is, the rate of increase in the exciton density matrix due to the absorption of light scattered on the grating. We shall restrict to the components that are diagonal in terms of the exciton wave vector $\boldsymbol{K}$,

$$g_{MM'}(\boldsymbol{K}) = 2\pi\hbar^{-1} V_{\boldsymbol{K},M} V^*_{\boldsymbol{K},M'}\ \delta(\hbar\omega - \mathcal{E}_{\rm exc}(\boldsymbol{K})). \quad (3)$$

Photons of the energy $\hbar\omega = \mathcal{E}_{\rm exc}(0)$ generate the excitons with $\boldsymbol{K} = 0$, and the related matrix elements $V_{0,\pm} \sim \boldsymbol{e}^*_\pm \cdot \boldsymbol{E}^0 = E^0_\pm$ are proportional to the circularly polarized components of the incident wave. In presence of the square lattice of symmetric NPs, the amplitude of the incident wave $\boldsymbol{E}^0$ is multiplied by the transmittance coefficient $t(\boldsymbol{K} = 0) = 1 + iq^2b^2\mathcal{X}/(2\pi n^2 q_{z,\boldsymbol{m}})$, which does not depend on the light polarization. Therefore, the lattice does not affect the optical orientation (and polarized luminescence) of excitons with $\boldsymbol{K} = 0$, and we can apply the phenomenological theory from [19] to outline this phenomenon. To calculate the generation of excitons by partially polarized light, the products of the amplitudes $E^0_\alpha E^{0*}_\beta$ in Eq. (3) are replaced with the components $d^0_{\alpha\beta}$ of the polarization matrix of incident radiation, which is convenient to represent in the basis of circular polarization vectors $\boldsymbol{e}_\pm$ in the form $d^0_{MM'} = I_0/2(\delta_{MM'} + \boldsymbol{\sigma}_{MM'}\cdot\boldsymbol{\mathcal{P}}^0)$. It involves the scalar product of the vector of Pauli matrices $\boldsymbol{\sigma} = (\sigma_x,\sigma_y,\sigma_z)$ and the vector of Stokes parameters of incident light $\boldsymbol{\mathcal{P}}^0 = (\mathcal{P}^0_l, \mathcal{P}^0_{l'}, \mathcal{P}^0_c)$. The latter are the degree of linear polarization in x, y axis, the degree of linear polarization in rotated by 45° x', y' axis, and the degree of circular polarization. Then the exciton generation matrix at $\boldsymbol{K} = 0$ coincides, up to a factor, with the polarization matrix in the circular basis [19]

$$g_{MM'}(\boldsymbol{K}) = \frac{g_0 I_0}{2} \begin{pmatrix} 1 + \mathcal{P}^0_c & \mathcal{P}^0_l - i\mathcal{P}^0_{l'} \\ \mathcal{P}^0_l + i\mathcal{P}^0_{l'} & 1 - \mathcal{P}^0_c \end{pmatrix} \times \delta(\boldsymbol{K})\,\delta(\hbar\omega - \mathcal{E}_{\rm exc}(0)). \quad (4)$$

It follows from Eq. (4) that the average spin of excitons in the moment of generation $\boldsymbol{M}^0 = \mathrm{Tr}(g\boldsymbol{\sigma})/\mathrm{Tr}(g)$ is equal to the vector $\boldsymbol{\mathcal{P}}^0$ that determines the polarization of incident light.

Combining Eqs. (2) and (3), we obtain the generation matrix for excitons with $\boldsymbol{K} \neq 0$,

$$g_{MM'}(\boldsymbol{K} \neq 0) = \sum_{\boldsymbol{m}} g_{\boldsymbol{m}} \left(\boldsymbol{e}^*_M \hat{G}_{\boldsymbol{b_m}} \boldsymbol{E}^0\right)\left(\boldsymbol{e}_{M'} \hat{G}^*_{\boldsymbol{b_m}} \boldsymbol{E}^{0*}\right) \times \delta(\boldsymbol{K} - \boldsymbol{b_m})\,\delta(\hbar\omega - \mathcal{E}_{\rm exc}(\boldsymbol{b_m})),$$

$$g_{\boldsymbol{m}} = (2\pi)^3\hbar^{-1}\left(\frac{ep_{\rm cv}}{m_0\omega_0}\right)^2 \left|\int \Phi^*(z-h)\, e^{iq_{z,\boldsymbol{m}}z} dz\right|^2 \times \left|\delta_{\boldsymbol{m},0} + \frac{iq^2b^2}{2\pi n^2 q_{z,\boldsymbol{m}}}\mathcal{X}\right|^2. \quad (5)$$

The contributions with $\boldsymbol{m} \neq 0$ are nonzero solely due to the grating, and the spin polarization of generated excitons is determined by the scattered waves $\boldsymbol{E}_{\boldsymbol{m}} \sim \hat{G}(\boldsymbol{b_m})\boldsymbol{E}^0$. Consider the incoming photons with the energy $\hbar\omega = \mathcal{E}_{\rm exc}(0) + \hbar^2b^2/2M_{\rm exc}$, such that the excitons with wave vectors $\boldsymbol{K} = \pm b\boldsymbol{e}_x$ or $\pm b\boldsymbol{e}_y$ are generated due to the scattering (in the first diffraction order, see Fig. 3). For these values of $\boldsymbol{K}$ the nonzero components of the tensor $\hat{G}(\boldsymbol{K})$ are $G_{xx}(\pm b\boldsymbol{e}_x) = G_{yy}(\pm b\boldsymbol{e}_y) = \eta$ and $G_{yy}(\pm b\boldsymbol{e}_x) = G_{xx}(\pm b\boldsymbol{e}_y) = 1$, where the parameter $\eta = 1 - b^2/q^2$ is responsible for the change of polarization of the scattered field from the polarization of light incident on the grating. Namely, the component of the

electric field $\boldsymbol{E}^0$ parallel to the wave vector $\boldsymbol{K}$ is scaled η times relative to the perpendicular component of the field. We consider this circumstance in (5) and replace the products of the field components with the polarization matrix to find

$$
\begin{aligned}
g_{MM'}(\boldsymbol{K}) &= \sum_{\boldsymbol{b_m}} \tilde{g}_{MM'}(\boldsymbol{b_m})\, \delta(\boldsymbol{K}-\boldsymbol{b_m})\, I_0\delta(\hbar\omega - \mathcal{E}_{\rm exc}(b)),\\
\tilde{g}_{MM'}(\pm b\boldsymbol{e}_x) &= \frac{g_1}{4}\begin{pmatrix} 1+\eta^2+\mathcal{P}_l^0(\eta^2-1)+2\eta\mathcal{P}_c^0 & \eta^2-1+\mathcal{P}_l^0(\eta^2+1)-2i\eta\mathcal{P}_{l'}^0 \\ \eta^2-1+\mathcal{P}_l^0(\eta^2+1)+2i\eta\mathcal{P}_{l'}^0 & 1+\eta^2+\mathcal{P}_l^0(\eta^2-1)-2\eta\mathcal{P}_c^0 \end{pmatrix},\\
\tilde{g}_{MM'}(\pm b\boldsymbol{e}_y) &= \frac{g_1}{4}\begin{pmatrix} 1+\eta^2+\mathcal{P}_l^0(1-\eta^2)+2\eta\mathcal{P}_c^0 & 1-\eta^2+\mathcal{P}_l^0(\eta^2+1)-2i\eta\mathcal{P}_{l'}^0 \\ 1-\eta^2+\mathcal{P}_l^0(\eta^2+1)+2i\eta\mathcal{P}_{l'}^0 & 1+\eta^2+\mathcal{P}_l^0(1-\eta^2)-2\eta\mathcal{P}_c^0 \end{pmatrix}.
\end{aligned}
\tag{6}
$$

Equation (6) implies that excitons having four allowed wave vector values are produced at different rates $\mathrm{Tr}g(\boldsymbol{K})$ and with different average spins. We note that the product $I_0\delta(\hbar\omega - \mathcal{E}_{\rm exc}(K))$ in Eqs. (4)–(6) originates from the consideration of monochromatic light, and in general case it should be replaced by the spectral intensity of radiation $I_0(\mathcal{E}_{\rm exc}(K))$ with the required photon energy.

III. EXCITON DENSITY MATRIX

To calculate the characteristics of the recombination radiation of excitons, we require the stationary value of their density matrix $\rho_{MM'}(\boldsymbol{K})$ that is determined by the equation [20] (see also Chapter 3 of [21])

$$
-\frac{i}{\hbar}[\mathcal{H}_B,\rho] - \frac{\rho}{\tau} - \frac{\rho-\langle\rho\rangle_\varphi}{\tau_p} + \left(\frac{\partial\langle\rho\rangle_\varphi}{\partial t}\right)_{s.r.} + g(\boldsymbol{K}) = 0. \tag{7}
$$

We assume here that the density matrix has spin indices $M, M' = \pm 1$, but it is diagonal in the momentum $\hbar\boldsymbol{K}$ of exciton motion in the QW plane. This approximation is valid when the elastic scattering of quasiparticles by impurities is considered, and the density matrix is averaged over random locations of scattering centers [22]. The first term in Eq. (7) is responsible for the evolution of the exciton spin in an external magnetic field. We consider the longitudinal magnetic field B_z, in which case the Hamiltonian $\mathcal{H}_B = \frac{1}{2}\hbar\Omega\sigma_z$ describes the splitting $\hbar\Omega = g_\parallel\mu_{\rm B}B_z$ of states with $M = \pm 1$. Here $\mu_{\rm B}$ is the Bohr magneton and $g_\parallel$ is the effective longitudinal g factor of the exciton. The second term in (7) describes the recombination of excitons characterized by the lifetime τ. The third term represents the relaxation of exciton momentum due to the elastic scattering, which brings the density matrix towards its average $\langle\rho\rangle = \frac{1}{2\pi}\int_0^{2\pi}\rho(\boldsymbol{K})d\varphi$ over the direction of exciton momentum $\hbar\boldsymbol{K}$. We assume the momentum relaxation time τ_p to be the shortest, which substantially simplifies the general theory [23]. The term $(\partial\langle\rho\rangle/\partial t)_{\rm s.r.}$ describing the spin relaxation process is taken into account in the simplest form

$$
\begin{aligned}
\frac{\partial}{\partial t}(\langle\rho_{++}\rangle - \langle\rho_{--}\rangle)_{\rm s.r.} &= -\frac{\langle\rho_{++}\rangle - \langle\rho_{--}\rangle}{\tau_{s1}},\\
\frac{\partial}{\partial t}\langle\rho_{+-}\rangle_{\rm s.r.} &= -\frac{\langle\rho_{+-}\rangle}{\tau_{s2}},\\
\frac{\partial}{\partial t}\langle\rho_{-+}\rangle_{\rm s.r.} &= -\frac{\langle\rho_{-+}\rangle}{\tau_{s2}}.
\end{aligned}
\tag{8}
$$

Thus the averaged z component of the exciton spin $\langle M_z\rangle = (\langle\rho_{++}\rangle - \langle\rho_{--}\rangle)/\mathrm{Tr}\langle\rho\rangle$ is considered to vanish with rate τ_{s1}^{-1}, while perpendicular components of the exciton spin $\langle M_x\rangle = (\langle\rho_{+-}\rangle + \langle\rho_{-+}\rangle)/\mathrm{Tr}\langle\rho\rangle$ and $\langle M_y\rangle = i(\langle\rho_{+-}\rangle - \langle\rho_{-+}\rangle)/\mathrm{Tr}\langle\rho\rangle$ vanish with rate τ_{s2}^{-1}. Such phenomenological picture is not restricted to specific spin relaxation mechanism, as it refers to the spin averaged over the exciton momentum orientation.

In this section, we do not take into account relaxation of the exciton's energy due to inelastic scattering, and seek the spin density matrix for constant values of energy and, naturally, $|\boldsymbol{K}|$. The secondary radiation of such excitons has the same frequency as the incident light.

To solve Eq. (7), we average it over the orientation of the wave vector $\boldsymbol{K}$, obtain the average density matrix and substitute it back into Eq. (7). It is convenient to present the spin density matrix in the form $\rho_{MM'} = N/2(\delta_{MM'} + \boldsymbol{\sigma}_{MM'}\cdot\boldsymbol{M})$, where $N = \mathrm{Tr}\rho$ is the number of excitons with the given wave vector, and $\boldsymbol{M} = \mathrm{Tr}(\rho\boldsymbol{\sigma})/N$ is the average angular momentum per exciton. The similar expansion was previously introduced for the matrix of light polarization and the matrix of exciton generation at $\boldsymbol{K} = 0$. The angular momentum components $M_{x,y}$ and M_z evolve independently, even as the spin relaxation (8) is included. However, the term $-i\hbar^{-1}[\mathcal{H}_B,\rho] = \Omega N(\sigma_y M_x - \sigma_x M_y)$ mixes the components in the QW plane, which corresponds to the spin precession in magnetic field B_z. Then after averaging Eq. (7) we find

$$
\begin{aligned}
\langle N\rangle &= \tau\ \mathrm{Tr}\langle g\rangle, \quad \langle NM_z\rangle = \tau_1\langle g_{++} - g_{--}\rangle,\\
\langle N(M_x - iM_y)\rangle &= \frac{\tau_2}{1+i\Omega\tau_2}\,2\langle g_{+-}\rangle,\\
\langle N(M_x + iM_y)\rangle &= \frac{\tau_2}{1-i\Omega\tau_2}\,2\langle g_{-+}\rangle.
\end{aligned}
\tag{9}
$$

Here $\tau_i^{-1} = \tau^{-1} + \tau_{si}^{-1}$ are the summary decay rates of the average exciton spin components. Next, we substitute the obtained averaged spin components back into (7) and designate $\tau_*^{-1} = \tau^{-1} + \tau_p^{-1}$ to find the result

$$
\begin{aligned}
N &= \tau_*\left(\mathrm{Tr}g + \frac{\tau}{\tau_p}\mathrm{Tr}\langle g\rangle\right),\\
NM_z &= \tau_*\left(g_{++} - g_{--} + \frac{\tau_1}{\tau_p}\langle g_{++} - g_{--}\rangle\right),
\end{aligned}
$$

$$N(M_x - iM_y) = \frac{2\tau_*}{1+i\Omega\tau_*}\left(g_{+-} + \frac{\tau_2}{\tau_p}\frac{\langle g_{+-}\rangle}{1+i\Omega\tau_2}\right) = N(M_x + iM_y)^*. \quad (10)$$

Since we obtained the exciton generation matrix (6) in the form $g(\boldsymbol{K}) = \sum_{|\boldsymbol{b_m}|=b} I_0\ \tilde{g}(\boldsymbol{b_m})\delta(\boldsymbol{K} - \boldsymbol{b_m})$, its average value over the direction of wave vector is $\langle g(\boldsymbol{K})\rangle = (\tilde{g}(b\boldsymbol{e}_x) + \tilde{g}(b\boldsymbol{e}_y))\ I_0/(\pi b)\ \delta(K - b)$. Therefore, the resulting density (10) includes contributions with the selected values of wave vector, proportional to the matrices $\tilde{g}(\boldsymbol{b_m})$, and the isotropic contribution proportional to the average matrix $(\tilde{g}(b\boldsymbol{e}_x) + \tilde{g}(b\boldsymbol{e}_y))/2$. In the case of rapid momentum relaxation, the isotropic contribution is dominant as $\tau_i \sim \tau \gg \tau_p$. Then we may simplify the result, considering $\tau_* \approx \tau_p$ and $\Omega\tau_p \ll 1$. After inserting the explicit generation matrix (6) in (10), we get the isotropic component of the density of excitons with $|\boldsymbol{K}| = b$ and their average spin

$$N = (\eta^2+1)\frac{\tau g_1 I_0}{\pi b}\delta(K-b), \quad M_z = \frac{\tau_1}{\tau}\frac{2\eta}{\eta^2+1}\mathcal{P}_c^0,$$
$$M_x - iM_y = \frac{1}{1+i\Omega\tau_2}\frac{\tau_2}{\tau}\left(\mathcal{P}_l^0 - i\frac{2\eta}{\eta^2+1}\mathcal{P}_{l'}^0\right). \quad (11)$$

This result should be compared to the orientation of excitons at $\boldsymbol{K} = 0$, for which an equation of the same kind (7) is applicable, except for the term corresponding to momentum relaxation [19]. In that case, given the generation matrix (4), we obtain the exciton density $N = \tau g_0 I_0\ \delta(\boldsymbol{K})$ and average spin components

$$M_z = \frac{\tau_1}{\tau}\mathcal{P}_c^0, \quad M_x - iM_y = \frac{1}{1+i\Omega\tau_2}\frac{\tau_2}{\tau}\left(\mathcal{P}_l^0 - i\mathcal{P}_{l'}^0\right). \quad (12)$$

Thus, when excitons with $|\boldsymbol{K}| = b$ are generated through the lattice of nanoparticles, the degrees of the circular and linear polarization in the axes x', y' rotated by 45° with respect to the lattice are multiplied by the factor $2\eta/(\eta^2+1)$. As in the case of $\boldsymbol{K} = 0$, circularly polarized light produces excitons whose spin is oriented along the z axis, and linearly polarized light generates excitons with spin in the perpendicular plane xy. However, we note that the lifetime τ and spin relaxation time τ_i entering Eqs. (11) and (12) generally are not the same for excitons with $|\boldsymbol{K}| = b$ or $\boldsymbol{K} = 0$. The degrees of the linear polarization $\mathcal{P}_l^0$ and $\mathcal{P}_{l'}^0$ enter the result (11) differently, since we have considered the generation of the excitons whose wave vectors are oriented along the lattice axes x, y. On the contrary, if the excitons with wave vectors $\boldsymbol{K} = b(\boldsymbol{e}_x \pm \boldsymbol{e}_y)$ are considered, the polarization degree $\mathcal{P}_{l'}^0$ will appear with the factor 1, and the polarization degree $\mathcal{P}_l^0$ will be multiplied by $2\eta'/(\eta'^2+1)$, where $\eta' = 1 - 2b^2/q^2$. In other words, the lattice does not alter the linear polarization in the axes that coincide with the directions of propagation of generated excitons.

IV. LUMINESCENCE OF HOT EXCITONS

In the previous section, we have calculated the distribution of excitons over momentum and their spin density matrix resulting from the continuous photogeneration. Now we look into the characteristics of the excitons' radiation, and we apply the Fermi golden rule to calculate the probability of spontaneous photon emission [24], since the exciton recombination occurs via nonradiative processes predominantly. The luminescence process, being inverse to the absorption of light, is characterized by the complex conjugate of the matrix element (2), where the external electric field $\boldsymbol{E}_0$ should be replaced with the field of the ground state of the selected photon mode. The photon modes in the considered structure (Fig. 1) differ from the photons in homogeneous medium, though both are described by the wave vector $\boldsymbol{q} = (\boldsymbol{q}_\parallel, q_z)$ and polarization (s or p) of the wave incident on the grating from the surrounding space. The radiation with a given frequency ω and wave vector $\boldsymbol{q}_\parallel$, detected at $z = -\infty$, includes both modes with $q_z = \pm(q^2 - q_\parallel^2)^{1/2}$. As shown in Fig. 3, the grating allows the luminescence of excitons whose wave vector lies in the regions $|\boldsymbol{K} - \boldsymbol{b_m}| = |\boldsymbol{q}_\parallel| < q(\omega)$, where the radiation wave vector $\boldsymbol{q}_\parallel$ can take any values inside the "light cone". Up to a constant that determines the intensity of radiation, the polarization matrix of the emitted wave is given by the following expression:

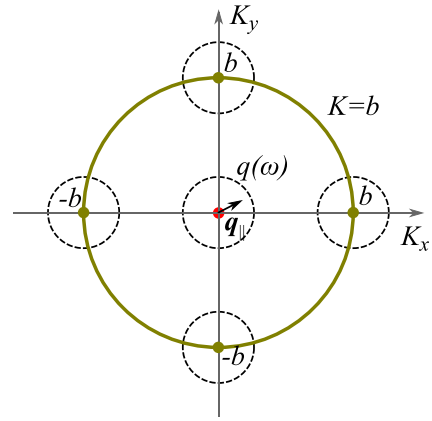

FIG. 3. Distribution in $\boldsymbol{K}$ space of the excitons generated by the light with the frequency $\omega = \omega_{\rm exc}(b)$. Dashed circles indicate the regions $|\boldsymbol{K} - \boldsymbol{b_m}| = |\boldsymbol{q}_\parallel| < q(\omega)$ of "bright" excitons that can emit photons with in-plane wave vector $\boldsymbol{q}_\parallel$.

$$d_{\alpha\beta}(\boldsymbol{q}_\parallel) = \sum_{\boldsymbol{K},MM'} V_{\boldsymbol{K},M;\boldsymbol{q}_\parallel,\alpha} V^*_{\boldsymbol{K},M';\boldsymbol{q}_\parallel,\beta}\ \rho_{MM'}(\boldsymbol{K}). \quad (13)$$

Next we consider the exciton radiation at small angles to the growth axis z, such that, on the one hand, this radiation can be distinguished from the specular reflection of the pump beam, and on the other hand, we can assume $\boldsymbol{q}_\parallel \approx 0$ and use the conjugate of Eq. (2) for the matrix element of the interaction operator. Substituting into (13) the density matrix of generated excitons with $|\boldsymbol{K}| = b$ defined by the parameters (11), and summing the contributions of the excitons with wave vectors $\boldsymbol{K} = \pm b\boldsymbol{e}_x$ and $\pm b\boldsymbol{e}_y$, we obtain the Stokes parameters of secondary radiation (which has the same frequency as the pump)

$$\mathcal{P}_l = \frac{\tau_2}{\tau}[1 + (\Omega\tau_2)^2]^{-1}\left(\mathcal{P}_l^0 - \Omega\tau_2\frac{2\eta}{\eta^2+1}\mathcal{P}_{l'}^0\right),$$
$$\mathcal{P}_{l'} = \frac{\tau_2}{\tau}[1 + (\Omega\tau_2)^2]^{-1}\frac{2\eta}{\eta^2+1}\left(\frac{2\eta}{\eta^2+1}\mathcal{P}_{l'}^0 + \Omega\tau_2\mathcal{P}_l^0\right),$$
$$\mathcal{P}_c = \frac{\tau_1}{\tau}\left(\frac{2\eta}{\eta^2+1}\right)^2\mathcal{P}_c^0. \quad (14)$$

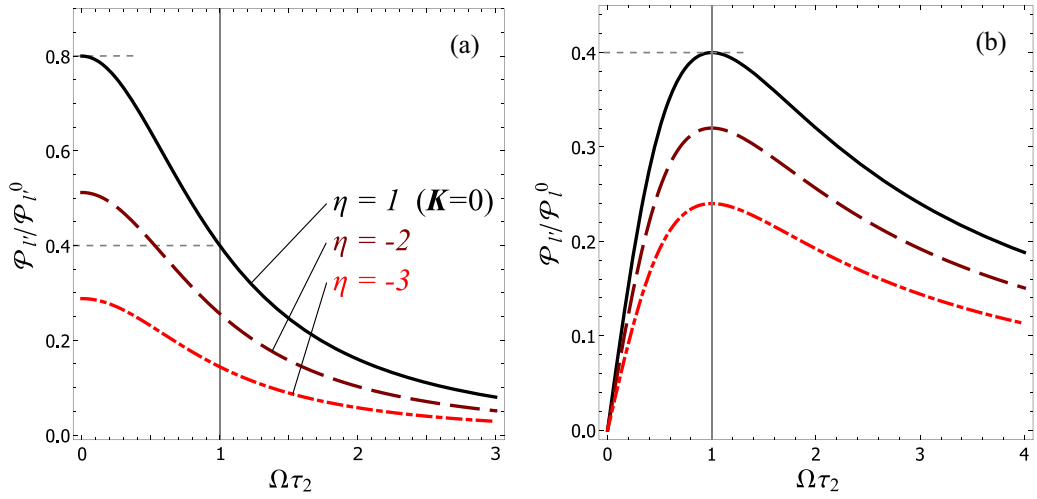

FIG. 4. Ratio of the linear polarization of exciton luminescence $\mathcal{P}_{l'}$ in the rotated x', y' axes to the linear polarization of the pump $\mathcal{P}_{l'}^0$ in the same axes (a), and to the linear polarization of the pump $\mathcal{P}_l^0$ in the x, y axes (b). Calculated from Eq. (14) with $\tau_2/\tau = 0.8$ as the function of parameter $\Omega\tau_2$ proportional to the magnetic field. Solid lines ($\eta = 1$) correspond to the conventional optical alignment of excitons with $\boldsymbol{K} = 0$. Dashed lines ($\eta = -2$) and dash-dotted lines ($\eta = -3$) demonstrate the effect of the grating. The indicated characteristic points of the plots are used to determine the spin relaxation time τ_2 from experiment.

In order to describe the luminescence of excitons with $\boldsymbol{K} = 0$, one could either substitute their spin density matrix (12) into Eq. (13), or formally set $\eta \to 1$ in Eq. (14). Either method yields the known result [1],

$$\mathcal{P}_l - i\mathcal{P}_{l'} = \frac{\tau_2}{\tau}\frac{1}{1+i\Omega\tau_2}\left(\mathcal{P}_l^0 - i\mathcal{P}_{l'}^0\right), \quad \mathcal{P}_c = \frac{\tau_1}{\tau}\mathcal{P}_c^0. \quad (15)$$

As seen from Eqs. (14) and (15), the circular polarization of luminescence reduces (compared to the pump polarization) due to the longitudinal spin relaxation. The linear polarization is reduced by the transverse spin relaxation, and further suppressed by the applied magnetic field. Additionally, in magnetic field the linear polarization of the pump $\mathcal{P}_l^0$ is partially transformed into the linear polarization of the luminescence $\mathcal{P}_{l'}$ in rotated axes (and vice versa, the polarization $\mathcal{P}_{l'}^0$ is converted into $\mathcal{P}_l$).

The difference in the polarized luminescence of excitons with $\boldsymbol{K} = 0$ and $|\boldsymbol{K}| = b$ is the lattice induced factor $2\eta/(\eta^2 + 1)$, which should not be too small so that the orientation of hot excitons could be observed. For that, the lattice period a should be only several times less (2–3 times) that the wavelength of light in semiconductor. Figure 4 shows the ratios of the linear polarization degrees of exciton luminescence and pump plotted as the functions of the parameter $\Omega\tau_2$ (proportional to magnetic field) for several values of the lattice parameter η. Measuring such dependencies (as in the Hanle effect) provides the estimations of the lifetime and spin relaxation time of excitons, but in the case $\eta \neq 1$, when the lattice is present, these times relate to hot excitons with nonzero wave vectors. Therefore, fabrication of a hybrid structure including a QW and a lattice of NPs will make it possible to study the properties of hot excitons.

V. SOLUTION OF KINETIC EQUATION INCLUDING EXCITON ENERGY RELAXATION

In the picture considered above, frequencies of the incident and emitted light coincide, which may hamper the observation of the polarized luminescence of hot excitons. However, these excitons are able to lose their kinetic energy while scattering on acoustic phonons, and then emit light on a lower frequency, which is shown schematically in Fig. 5. To describe the orientation of exciton spin in this case, it is necessary to include the energy relaxation in Eq. (7) for the stationary density matrix. It can be accomplished using the equation of the Fokker-Planck type [25], assuming that the kinetic energy of exciton changes in relatively small portions as it interacts with long-wave acoustic phonons. Considering the spontaneous emission of phonons to be dominant over absorption, we neglect the energy diffusion term and write the equation for the exciton density matrix $\langle\rho\rangle$ averaged over the

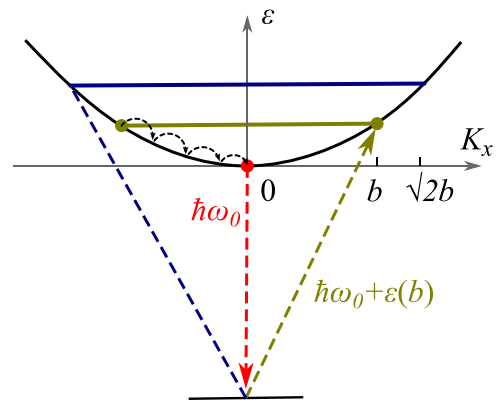

FIG. 5. Schematic of excitation and radiative recombination of excitons, taking into account their energy relaxation caused by the emission of acoustic phonons.

momentum orientations,

$$-\frac{i\Omega}{2\hbar}[\sigma_z, \langle\rho\rangle] - \frac{\langle\rho\rangle}{\tau} + \left(\frac{\partial\langle\rho\rangle}{\partial t}\right)_{\text{s.r.}} + \frac{\partial}{\partial\varepsilon}\left(\frac{\varepsilon}{\tau_\varepsilon}\langle\rho\rangle\right) + \langle g\rangle = 0. \tag{16}$$

Compared to Eq. (7), here the almost immediate momentum relaxation is taken into account, and the density matrix $\langle\rho\rangle(\varepsilon)$ depends only on the kinetic energy $\varepsilon(K) \approx \hbar^2K^2/(2M_{\text{exc}})$. The new penultimate term in Eq. (16) corresponds to the drift of excitons towards the lower kinetic energy. We present the exciton generation matrix averaged over momentum directions in the form $\langle g\rangle = 1/2\ \text{Tr}\langle g\rangle(1 + \boldsymbol{\sigma}\cdot\boldsymbol{M}^0)$. For excitation in a narrow spectral range $\text{Tr}\langle g\rangle = \mathcal{G}\ \delta(\varepsilon - \varepsilon_0)$, so that excitons with a certain kinetic energy value ε_0 are generated. For example, in case of the excitons with wave vectors $\boldsymbol{K} = \pm b\boldsymbol{e}_x$ and $\pm b\boldsymbol{e}_y$ we have $\varepsilon_0 = \varepsilon(b)$, and averaging Eq. (6) yields $\mathcal{G} = (\eta^2 + 1)g_1I_0\hbar^2/(2\pi M_{\text{exc}})$ and the average exciton spin at the moment of generation $\boldsymbol{M}^0 = (\mathcal{P}_l^0, 2\eta/(\eta^2 + 1)\mathcal{P}_{l'}^0, 2\eta/(\eta^2 + 1)\ \mathcal{P}_c^0)$.

To solve Eq. (16), again we use the representation of the density matrix $\langle\rho\rangle = N/2\ (1 + \boldsymbol{\sigma}\cdot\boldsymbol{M})$, and obtain a system of equations for concentration and mean angular momentum projections (which are now regarded as functions of ε),

$$\frac{N}{\tau} - \frac{\partial}{\partial\varepsilon}\left(\frac{\varepsilon}{\tau_\varepsilon}N\right) = \mathcal{G}\ \delta(\varepsilon - \varepsilon_0), \tag{17}$$

$$\frac{NM_z}{\tau_1} - \frac{\partial}{\partial\varepsilon}\left(\frac{\varepsilon}{\tau_\varepsilon}NM_z\right) = \mathcal{G}M_z^0\ \delta(\varepsilon - \varepsilon_0), \tag{18}$$

$$\left[\frac{1}{\tau_2} + i\Omega - \frac{\partial}{\partial\varepsilon}\frac{\varepsilon}{\tau_\varepsilon}\right]N(M_x - iM_y) = \mathcal{G}\left(M_x^0 - iM_y^0\right)\ \delta(\varepsilon - \varepsilon_0). \tag{19}$$

The last equation is valid together with its complex conjugate. The equations with δ functions on the right-hand side are equivalent to the homogeneous ones in the range $0 < \varepsilon < \varepsilon_0$ with boundary conditions $N(\varepsilon_0 - 0) = \mathcal{G}\ \tau_\varepsilon(\varepsilon_0)/\varepsilon_0$ and $NM_i(\varepsilon_0 - 0) = \mathcal{G}M_i^0\ \tau_\varepsilon(\varepsilon_0)/\varepsilon_0$ that suggest the absence of excitons with energies $\varepsilon > \varepsilon_0$. Their solution is

$$N(\varepsilon) = \mathcal{G}\ \frac{\tau_\varepsilon}{\varepsilon}\ \exp\left(-\int_\varepsilon^{\varepsilon_0}\frac{d\varepsilon'}{\varepsilon'}\frac{\tau_\varepsilon}{\tau}\right), \tag{20}$$

$$NM_z = \mathcal{G}M_z^0\ \frac{\tau_\varepsilon}{\varepsilon}\ \exp\left(-\int_\varepsilon^{\varepsilon_0}\frac{d\varepsilon'}{\varepsilon'}\frac{\tau_\varepsilon}{\tau_1}\right), \tag{21}$$

and, if the notation $T = \int_\varepsilon^{\varepsilon_0} d\varepsilon'\tau_\varepsilon/\varepsilon'$ is introduced, the transverse components of angular momentum are given by the following equation and its complex conjugate:

$$N(M_x - iM_y) = \mathcal{G}\left(M_x^0 - iM_y^0\right)\frac{\tau_\varepsilon}{\varepsilon} \times \exp\left(-\int_\varepsilon^{\varepsilon_0}\frac{d\varepsilon'}{\varepsilon'}\frac{\tau_\varepsilon}{\tau_2} - i\Omega T\right). \tag{22}$$

Integrals in Eqs. (20)–(22) can be estimated by assuming the lifetimes τ, $\tau_\varepsilon = \text{const}(\varepsilon)$ to be independent of the kinetic energy, and the spin relaxation time $\tau_{si}(\varepsilon) \sim \varepsilon^{-1}$, which is valid in case of the Dyakonov-Perel mechanism of spin relaxation [26]. Recollecting the notation $\tau_i^{-1} = \tau^{-1} + \tau_{si}^{-1}$, we obtain the functions of energy

$$N(\varepsilon) = \mathcal{G}\ \frac{\tau_\varepsilon}{\varepsilon}\left(\frac{\varepsilon}{\varepsilon_0}\right)^{\tau_\varepsilon/\tau}, \tag{23}$$

$$M_z = M_z^0 \exp\left(\frac{\tau_\varepsilon}{\tau_{s1}(\varepsilon)} - \frac{\tau_\varepsilon}{\tau_{s1}(\varepsilon_0)}\right), \tag{24}$$

$$M_x - iM_y = \left(M_x^0 - iM_y^0\right)\exp\left(\frac{\tau_\varepsilon}{\tau_{s2}(\varepsilon)} - \frac{\tau_\varepsilon}{\tau_{s2}(\varepsilon_0)}\right) \times \exp(-i\Omega T). \tag{25}$$

Therefore, as excitons lose their kinetic energy, their spin component M_z decreases exponentially, the steeper the longer the energy relaxation time τ_ε. Transverse spin components diminish as well when the exciton energy decreases, and additionally transform into each other due to the spin precession with frequency Ω in applied magnetic field. However, in contrast to the result (11) obtained in absence of the energy relaxation, Eq. (25) lacks the factor $(1 + i\Omega\tau_2)^{-1}$ that ensures the decreasing dependence of the transverse spin components on the magnetic field. It should be emphasized that Eqs. (11) and (23)–(25) relate to essentially different pictures. The former considers the polarization of excitons that had not yet lost their energy, while the latter ones refer to the excitons with lower kinetic energy that originate exactly from the relaxation process. Some excitons, having lost their kinetic energy by emitting phonons, end up near the bottom of the Brillouin zone and radiate light at the frequency $\omega \approx \omega_0$. According to Eq. (13), the polarization of luminescence of these excitons, observed along the z axis, is equal to the average spin components that are given by Eqs. (24) and (25) at $\varepsilon \to 0$. Thus, the nanoparticle grating makes it possible to generate the hot excitons via the absorption of photons with energies $\hbar\omega = \mathcal{E}_{\text{exc}}(\boldsymbol{b_m})$, and detect the luminescence of the thermalized excitons with $\boldsymbol{K} = 0$, which provides the information about the kinetics of relaxation processes.

VI. CONCLUSIONS

The paper theoretically considers the optical orientation of hot excitons in a QW that are generated with the near field of a grating of metal nanoparticles embedded in semiconductor heterostructure. A model is developed to consider the effect of the grating on the exciton spin orientation and polarization of the exciton luminescence. It is demonstrated that gratings of a period several times smaller than the wavelength of exciting light preserve the correlation between the polarizations of the exciton luminescence and the pumping beam. This enables the experimental determination of the lifetime and spin relaxation time of hot excitons via the measurement of the degrees of circular and linear polarization of secondary radiation in applied magnetic field. Apart from the quasiresonant luminescence, the radiation occurs on the lower frequencies due to the relaxation of exciton's kinetic energy. The dependence of the polarization of luminescence of thermalized excitons on magnetic field in the Faraday geometry provides insight into the kinetics of relaxation process.

ACKNOWLEDGMENT

This work was supported by the Russian Science Foundation, Project No. 22-12-00139.

[1] G. E. Pikus and E. L. Ivchenko, Optical orientation and polarized luminescence of excitons in semiconductors, in *Excitons*, edited by E. I. Rashba and M. D. Sturge (North-Holland, Amsterdam, 1982).

[2] R. Planel and C. Benoit a la Guillaume, Optical orientation of excitons, in *Optical Orientation*, edited by F. Meier and B. P. Zakharchenya (North-Holland, Amsterdam, 1984).

[3] E. M. Gamarts, E. L. Ivchenko, M. I. Karaman, V. P. Mushinskii, G. E. Pikus, B. S. Razbirin, and A. N. Starukhin, Optical orientation and alignment of free excitons in GaSe during resonance excitation. Experiment., Sov. Phys. JETP **46**, 590 (1977).

[4] R. I. Dzhioev, H. M. Gibbs, E. L. Ivchenko, G. Khitrova, V. L. Korenev, M. N. Tkachuk, and B. P. Zakharchenya, Determination of interface preference by observation of linear-to-circular polarization conversion under optical orientation of excitons in type-II GaAs/AlAs superlattices, Phys. Rev. B **56**, 13405 (1997).

[5] O. O. Smirnova, I. V. Kalitukha, A. V. Rodina, G. S. Dimitriev, V. F. Sapega, O. S. Ken, V. L. Korenev, N. V. Kozyrev, S. V. Nekrasov, Y. G. Kusrayev *et al.*, Optical alignment and optical orientation of excitons in CdSe/CdS colloidal nanoplatelets, Nanomaterials **13**, 2402 (2023).

[6] G. L. Bir, E. L. Ivchenko, and G. E. Pikus, Alignment and orientation of hot excitons and polarized luminescence, Bull. Acad. Sci. USSR, Phys. Ser. **40**, 81 (1976).

[7] P. Vasa, R. Pomraenke, S. Schwieger, Y. I. Mazur, V. Kunets, P. Srinivasan, E. Johnson, J. E. Kihm, D. S. Kim, E. Runge, G. Salamo, and C. Lienau, Coherent exciton-surface-plasmon-polariton interaction in hybrid metal-semiconductor nanostructures, Phys. Rev. Lett. **101**, 116801 (2008).

[8] I. A. Akimov, A. N. Poddubny, J. Vondran, Y. V. Vorobyov, L. V. Litvin, R. Jede, G. Karczewski, S. Chusnutdinow, T. Wojtowicz, and M. Bayer, Plasmon-to-exciton spin conversion in semiconductor-metal hybrid nanostructures, Phys. Rev. B **103**, 085425 (2021).

[9] B. J. Lawrie, K.-W. Kim, D. P. Norton, and R. F. Haglund, Jr., Plasmon-exciton hybridization in ZnO quantum-well Al nanodisc heterostructures, Nano Lett. **12**, 6152 (2012).

[10] N. S. Averkiev, A. V. Korotchenkov, and V. A. Kosobukin, On the theory of plasmon–Excitons: An estimate of the coupling constant and the optical spectrum, Semiconductors **53**, 1042 (2019).

[11] M. Pelton, S. D. Storm, and H. Leng, Strong coupling of emitters to single plasmonic nanoparticles: Exciton-induced transparency and Rabi splitting, Nanoscale **11**, 14540 (2019).

[12] T. Hu, Y. Wang, L. Wu, L. Zhang, Y. Shan, J. Lu, J. Wang, S. Luo, Z. Zhang, L. Liao, S. Wu, X. Shen, and Z. Chen, Strong coupling between Tamm plasmon polariton and two dimensional semiconductor excitons, Appl. Phys. Lett. **110**, 051101 (2017).

[13] B. W. Li, S. Zu, Z. P. Zhang, L. H. Zheng, Q. Jiang, B. W. Du, Y. Luo, Y. J. Gong, Y. F. Zhang, F. Lin *et al.*, Large Rabi splitting obtained in Ag-WS2 strong-coupling heterostructure with optical microcavity at room temperature, Opto-Electron. Adv. **2**, 190008 (2019).

[14] F. J. García De Abajo, *Colloquium:* Light scattering by particle and hole arrays, Rev. Mod. Phys. **79**, 1267 (2007).

[15] E. L. Ivchenko, *Optical Spectroscopy of Semiconductor Nanostructures* (Alpha Science International, Harrow, UK, 2005).

[16] R. I. Dzhioev, B. P. Zakharchenya, E. L. Ivchenko, V. L. Korenev, Y. G. Kusraev, N. N. Ledentsov, V. M. Ustinov, A. E. Zhukov, and A. F. Tsatsul'nikov, Optical orientation and alignment of excitons in quantum dots, Phys. Solid State **40**, 790 (1998).

[17] V. I. Sugakov and G. V. Vertsimakha, Localized exciton states with giant oscillator strength in quantum well in vicinity of metallic nanoparticle, Phys. Rev. B **81**, 235308 (2010).

[18] Y. Chen, Y. Zhang, and A. F. Koenderink, General point dipole theory for periodic metasurfaces: Magnetoelectric scattering lattices coupled to planar photonic structures, Opt. Express **25**, 21358 (2017).

[19] G. L. Bir and G. E. Pikus, Optical orientation of excitons in uniaxial crystals. Large exchange splitting, Sov. Phys. JETP **37**, 1116 (1973).

[20] E. L. Ivchenko and G. E. Pikus, *Superlattices and Other Heterostructures: Symmetry and Optical Phenomena*, Springer Series in Solid-State Sciences (Springer, Berlin, 1997), Vol. 110.

[21] H.-P. Breuer and F. Petruccione, *The Theory of Open Quantum Systems* (Oxford University Press, Oxford, 2002).

[22] W. Kohn and J. M. Luttinger, Quantum theory of electrical transport phenomena, Phys. Rev. **108**, 590 (1957).

[23] E. L. Ivchenko, G. E. Pikus, B. S. Razbirin, and A. N. Starukhin, Optical orientation and alignment of free excitons in GaSe under resonant excitation. Theory, Sov. Phys. JETP **45**, 1172 (1977).

[24] H. Barry Bebb and E. W. Williams, Photoluminescence I: Theory, in *Semiconductors and Semimetals*, edited by R. K. Willardson and A. C. Beer (Elsevier, Amsterdam, 1972), Vol. 8, pp. 181–320.

[25] V. N. Abakumov, V. I. Perel, and I. N. Yassievich, *Nonradiative Recombination in Semiconductors* (North-Holland, Amsterdam, 1991).

[26] I. A. Kokurin, P. V. Petrov, and N. S. Averkiev, Optical orientation of electrons in compensated semiconductors, Semiconductors **47**, 1232 (2013).